Recognition Science: Fundamental Physics from a Unique Comparison Law

Jonathan Washburn[a,1,*], Megan Simons[a,2], Recognition Science Team[a]

[a] *Recognition Physics Institute, Austin, Texas, USA*

Abstract

Recognition Science connects physical laws through the calibrated comparison cost $J(x) = (x+x^{-1})/2-1$. Assigning matter's kinetic energy to the field cost's Hessian gives a common functional whose variation fixes both propagation and coherence-dependent field response. On any finite connected simple graph, a unique field exists for every normalized state and static link configuration exactly when the graph has no bridge. With the stated coherent-time term, the resulting nonlinear evolution is global and conserves norm and energy. Trivial links give a unique positive ground state, a stable phase orbit, and an equilibrium operator with an exact transform to reversible probability transport. An explicit cubic example separates field response from density and instantaneous current. The same comparison law also connects constrained response to fluctuations, amplitudes to Born probabilities, geometric metric modes to light propagation, and charged currents to gauge response. Cosmological assignments yield linked dark-energy observables. Each physical realization retains its stated carrier, clock, and readout conditions.

Keywords: Reciprocal comparison cost, Coupled matter and field, Nonlinear dynamics, Ground-state stability, Discrete gravity, Cosmology

1. One rule, several physical readings

A physical theory must say what can change, how it changes, and what an instrument reads. Recognition Science assigns a cost to comparing two positive quantities. Their ratio x is dimensionless. Exchanging them sends x to x^{-1}, while equality is $x = 1$. The question is whether composing comparisons determines the cost itself.

The canonical reciprocal cost has a published uniqueness theorem [1]. Conserved comparison ledgers place this cost inside an explicit structural system, with separate hypotheses governing scale and readout [2, 3]. Published constructions further connect it to stable fields on graphs, normalized state amplitudes, unitary evolution, and a Newtonian gravitational limit [4, 5, 6]. The physics constructions assign the mathematical objects to records, spatial relations, and measured quantities. Those assignments are part of the physical theory and are stated with each application.

* Corresponding author.

Email address: `jon@recognitionphysics.org` (Jonathan Washburn)

[1] Jonathan Washburn ORCID: 0009-0001-8868-7497.

[2] Megan Simons ORCID: 0000-0001-9457-7019.

Term	Mathematical object	Physical reading
Comparison	Positive ratio x	Relative magnitude of two quantities
Cost	$J(x)$	Price assigned to imbalance
Posting	Oriented entry on a channel	One recorded transfer
Shared carrier	One variable per oriented channel	The same transfer can enter several constraints
Hinge	Codimension-two simplex	Location of discrete curvature
Readout	Map from a state to an observable	What an instrument records

The common law connects quantities that are often introduced separately. A single constrained Hessian controls both static response and Gaussian fluctuations. A single cost admits an exact state-amplitude realization. When the field Hessian also supplies matter's kinetic form, the same functional fixes both matter propagation and its backreaction on the field. Section 4 gives the exact graph criterion for global field solvability, proves a unique positive ground state and nonlinear orbital stability for trivial links, and solves a phase-dependent cubic example exactly. Its equilibrium operator also gives a reversible probability flow with the same stationary density. A single geometric spatial eigenvalue also fixes two propagation laws. Figure 1 locates the connections. Extending the finite coupled dynamics to the physical charged and geometric carriers requires their common clock, state identification, and observable normalization.

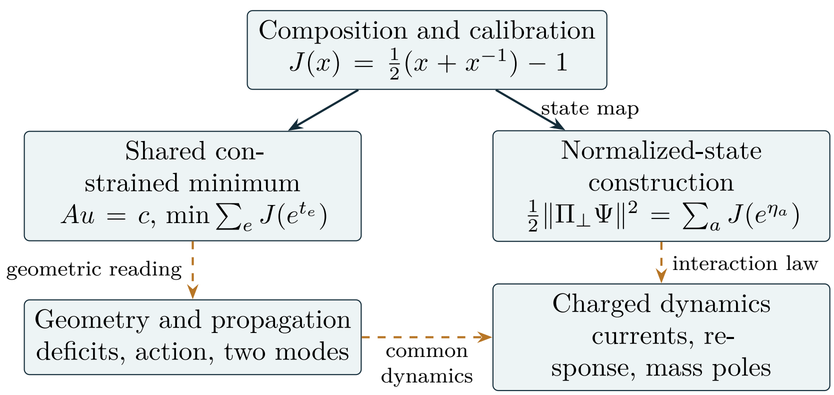

Figure 1: From one cost to coupled physical sectors. Solid arrows denote mathematical constructions under the displayed premises. Dashed arrows require a physical identification or interaction law. Section 4 gives an explicit finite matter–field coupling; its extension to the geometric and charged sectors retains the indicated identification steps. The normalized-state construction is proved in Section 5.3; its physical readout uses Section 5.4.

2. The comparison law

For $x, y > 0$, consider

$$F(xy) + F(x/y) = 2F(x)F(y) + 2F(x) + 2F(y). \tag{1}$$

In logarithmic coordinates, $H(t) = 1 + F(e^t)$ obeys

$$H(t+s) + H(t-s) = 2H(t)H(s). \tag{2}$$

The local quadratic calibration fixes the entire function, without assuming continuity or differentiability of the unknown cost.

Theorem 1 (Cost uniqueness from composition and local calibration)**.** *Let $F : (0, \infty) \to \mathbb{R}$ satisfy* (1) *and*

$$\lim_{\substack{t \to 0 \\ t \neq 0}} \frac{2F(e^t)}{t^2} = 1. \tag{3}$$

Then

$$F(x) = J(x) = \frac{x + x^{-1}}{2} - 1 = \frac{(x-1)^2}{2x}, \qquad J(e^t) = \cosh t - 1. \tag{4}$$

Normalization, reciprocity, nonnegativity, and smoothness follow from these two premises.

Proof. Setting $y = 1$ in (1) gives $F(1)[F(x) + 1] = 0$ for every $x > 0$. If $F(1) \neq 0$, then F is identically -1, contradicting (3). Thus $F(1) = 0$. With $H(t) = 1 + F(e^t)$, the diagonal case of (2) gives

$$H(2t) = 2H(t)^2 - 1, \qquad H(0) = 1.$$

Calibration gives $H(s) = 1 + s^2/2 + o(s^2)$ as $s \to 0$, so $H(s) > 1$ for sufficiently small nonzero s. Since $\operatorname{arcosh}(1+u)/\sqrt{2u} \to 1$ as $u \downarrow 0$,

$$\frac{\operatorname{arcosh} H(s)}{|s|} \longrightarrow 1.$$

Fix $t \neq 0$. For every sufficiently large n, repeated use of $2\cosh^2 v - 1 = \cosh(2v)$ gives

$$H(t) = \cosh\left(2^n \operatorname{arcosh} H(t/2^n)\right).$$

The argument tends to $|t|$, proving $H(t) = \cosh t$. The value at zero and $t = \log x$ complete the proof. The inverse-cosh limit used here follows by inverting $\cosh v = 1 + v^2/2 + o(v^2)$ for $v \geq 0$. □

The local calibration fixes the unit of comparison; the composition law carries it to every finite ratio. In the smooth case, the same mechanism is the initial-value problem $H'' = H$, $H(0) = 1$, $H'(0) = 0$, obtained by differentiating (2) twice. The reciprocal cost and its regularity connection are developed in [1].

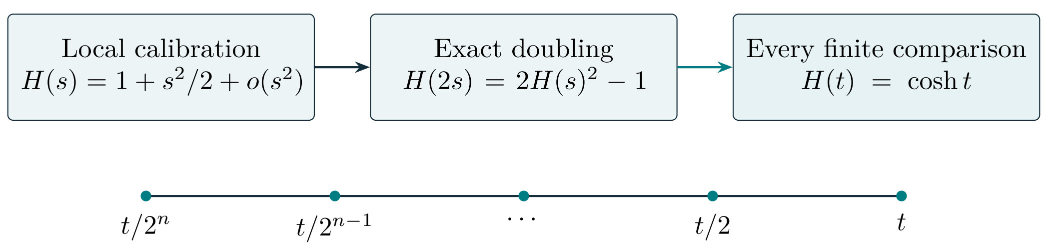

Halve into the calibrated neighborhood; double back by an exact identity.

Figure 2: Local information determines the global cost. Repeated halving reaches the quadratic regime at any fixed comparison, and exact doubling transports its calibrated value back. Regularity of the unknown function is a conclusion.

There is also a structural reason for the form of the composition law. Suppose F is continuous and nonconstant, $F(1) = 0$, and $F(xy) + F(x/y) = P(F(x), F(y))$ for a symmetric polynomial P of total degree at most two. Setting $y = 1$ gives $P(u, 0) = 2u$ on an interval in the range of F. Polynomial equality and symmetry leave only

$$P(u, v) = 2u + 2v + cuv.$$

This is the published d'Alembert classification [7]. Selecting $c = 2$ fixes the multiplicative coordinate used in (1). Unit logarithmic curvature alone would allow $F_\alpha(x) = \alpha^{-2}[\cosh(\alpha \log x) - 1]$ with $c = 2\alpha^2$; the coordinate normalization is therefore a separate input.

The scale hierarchy has its own structural input. Let positive levels obey $\ell_{n+1} = r\ell_n$ under the same update at every level, and let the least distinct binary join obey $\ell_2 = \ell_1 + \ell_0$. Then

$$r^2 = r + 1, \qquad r = \varphi = \frac{1+\sqrt{5}}{2}, \qquad \ell_n = \ell_0 \varphi^n.$$

The hierarchy theorem determines a ratio once those update and join conditions hold [8]. The spatial theorem uses another physical requirement: completed recognition is retained under motions that make no new posting. In its specified topological realization, the nontrivial linking detector selects three spatial dimensions [9]. The associated binary cube has $2^3 = 8$ vertices and $3\,2^2 = 12$ edges. The roles of the hierarchy and of spatial persistence remain distinct.

3. An exact interacting minimum

Two loops sharing an edge cannot minimize that edge independently. There is one edge variable. This elementary requirement produces a coupled variational problem even before a spacetime interpretation is chosen.

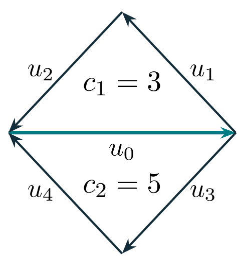

One shared edge, charged once.

$u_0 + u_1 + u_2 = 3$
$u_0 + u_3 + u_4 = 5$

At the unique minimum, $2 < u_0 < 3$. The unequal loop contents are compatible.

Figure 3: Interaction through shared incidence. The constraints refer to the same edge variable, so their responses are coupled. No uniform-curvature assumption is needed.

Let $A \in \mathbb{R}^{H \times E}$ be a finite signed incidence matrix, including traversal multiplicities, and let $c \in \operatorname{im} A$ be prescribed contents. Put

$$u_e = \sinh t_e, \qquad f(u) = \sqrt{1+u^2} - 1, \qquad W(c) = \min_{Au=c} \sum_e f(u_e). \tag{5}$$

Since $f(\sinh t) = J(e^t)$, this is precisely the reciprocal cost in a content coordinate. The following result is established in the gravity construction [10]; its proof is included because the common response is central here.

Theorem 2 (Shared content and response)**.** *For every compatible c, the minimum in (5) exists and is unique. Its optimizer satisfies*

$$\frac{u_e^*}{\sqrt{1+(u_e^*)^2}} = (A^T\lambda)_e, \qquad \tanh t_e^* = (A^T\lambda)_e. \tag{6}$$

If A has full row rank, W is analytic and

$$\nabla W = \lambda, \qquad \nabla^2 W = (AD^{-1}A^T)^{-1}, \qquad D = \operatorname{diag}_e(1+(u_e^*)^2)^{-3/2}. \tag{7}$$

In particular, $0 \prec \nabla^2 W \preceq (AA^T)^{-1}$.

Proof. The affine constraint is nonempty and closed. The bound $f(u) \geq |u| - 1$ makes every bounded sublevel set compact. Strict positivity of

$$f''(u) = (1+u^2)^{-3/2}$$

gives uniqueness. Stationarity along $\ker A$ places $\nabla F(u^*)$ in $\operatorname{im} A^T$, proving (6). Conversely the strict tangent inequality proves that any feasible stationary point is the unique minimum.

With full row rank, the linearization of $(\nabla F(u) - A^T\lambda, Au - c)$ is

$$\begin{pmatrix} D & -A^T \\ A & 0 \end{pmatrix}.$$

Its null vector (v, μ) obeys $v^T Dv = 0$, hence $v = 0$ and $\mu = 0$. The analytic implicit-function theorem and uniqueness give a global analytic optimizer. Differentiation gives $du = D^{-1}A^T d\lambda$ and $dc = AD^{-1}A^T d\lambda$. Also $dW = \lambda^T dc$. These prove (7). Finally $D^{-1} \succeq I$ implies the claimed bound by inversion of positive matrices. □

The off-diagonal response measures the effect of changing one loop on another through their shared channels. For a single loop with n distinct edges,

$$W(c) = n\left(\sqrt{1 + (c/n)^2} - 1\right), \quad W''(c) = \frac{1}{n}\left(1 + (c/n)^2\right)^{-3/2}.$$

The response softens continuously as content grows.

In Figure 3, fixing $x = u_0$ sets $u_1 = u_2 = (3 - x)/2$ and $u_3 = u_4 = (5 - x)/2$. The remaining stationarity equation is

$$G(x) = f'(x) - f'((3 - x)/2) - f'((5 - x)/2) = 0.$$

Its derivative is positive. Since $G(2) = 1/\sqrt{5} - 3/\sqrt{13} < 0$ and $G(3) = 3/\sqrt{10} - 1/\sqrt{2} > 0$, its unique solution lies between two and three.

3.1. Response and fluctuations are the same operator

The constraint response in (7) concerns changes in the prescribed contents. A source applied to the channels probes the complementary response at fixed contents. Both follow from the same Hessian.

Theorem 3 (Constrained response–fluctuation identity)**.** *Let A have full row rank, fix c, and write $F(u) = \sum_e f(u_e)$. For $\|b\|_\infty < 1$, let $u(b)$ minimize $F(u) - b^T u$ subject to $Au = c$. At $b = 0$, put $D = \nabla^2 F(u^*)$ and define*

$$K = D^{-1} - D^{-1}A^T(AD^{-1}A^T)^{-1}AD^{-1}. \tag{8}$$

Then

$$\begin{gathered} \left.\frac{\partial u}{\partial b}\right|_0 = K, \qquad \operatorname{Cov}_{\nu_\beta}(\xi) = \frac{K}{\beta}, \\ d\nu_\beta(\xi) \propto e^{-\beta\xi^T D\xi/2}\, d\xi, \qquad \xi \in \ker A, \end{gathered} \tag{9}$$

where $\beta > 0$ and $d\xi$ is Euclidean volume on $\ker A$. Moreover $K \succeq 0$, $AK = 0$, and $\operatorname{rank} K = E - H$.

Proof. Since $F(u) - b^T u \geq (1 - \|b\|_\infty)\|u\|_1 - E$, a unique minimizer exists. The implicit-function theorem applies by the invertible linearization in Theorem 2. Differentiating $\nabla F(u) - b = A^T\lambda$ and $Au = c$ gives

$$D\, du - db = A^T d\lambda, \qquad A\, du = 0.$$

Solving these equations gives $du = K\, db$. Let the columns of Q be an orthonormal basis of $\ker A$. The Gaussian coordinate $\xi = Qz$ has covariance

$$\beta^{-1}Q(Q^T DQ)^{-1}Q^T.$$

Both Kb and $Q(Q^T DQ)^{-1}Q^T b$ are the unique $x \in \ker A$ satisfying $Q^T Dx = Q^T b$, so the matrices agree. Positivity, the constraint identity, and the rank follow from this representation. When $E = H$, the tangent space is zero and both responses vanish. □

Both responses are blocks of one inverse. With $S = AD^{-1}A^T$, direct multiplication gives

$$\begin{pmatrix} D & -A^T \\ A & 0 \end{pmatrix}^{-1} = \begin{pmatrix} K & D^{-1}A^T S^{-1} \\ -S^{-1}AD^{-1} & S^{-1} \end{pmatrix}. \tag{10}$$

The upper diagonal block is $K = \beta\,\mathrm{Cov}(\xi)$, the lower one is $S^{-1} = \nabla^2 W$, and the off-diagonal block gives $du/dc = D^{-1}A^T S^{-1}$. Thus imposed content, channel response, and tangent fluctuations are tied by the same constrained Hessian.

This is an exact connection between response and quadratic fluctuations of the same interacting system. It does not replace the full nonlinear finite-temperature covariance or specify a Lorentzian propagator. The nonlinear minimum nevertheless has a controlled quartic approximation with a global error bound, derived in Appendix A.

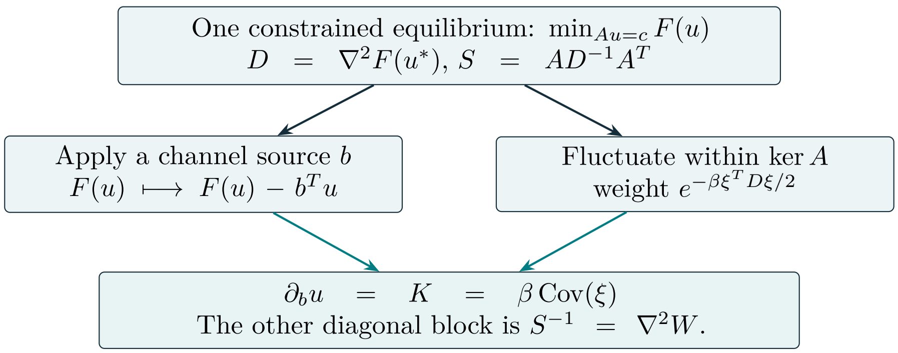

Figure 4: A common action fixes both responses. The covariance is taken on the allowed tangent space, so constrained directions cannot fluctuate. No independent covariance matrix is fitted.

3.2. Stable fields and conserved flux

The logarithmic coordinate gives another useful realization of the same cost. On a finite connected graph with at least two vertices, let d take vertex values to oriented edge differences and let h be a fixed edge field. The published flux-sector construction [4] uses

$$E_h(v) = \sum_e [\cosh(h_e + (dv)_e) - 1].$$

Fixing the mean of v gives a unique minimizer v_h. If λ_2 is the first nonzero eigenvalue of $d^T d$, then

$$d^T \sinh(h + dv_h) = 0, \qquad E_h(v_h + \eta) - E_h(v_h) \geq \tfrac{1}{2}\|d\eta\|^2 \geq \tfrac{\lambda_2}{2}\|\eta - \bar{\eta}\|^2. \tag{11}$$

Indeed the Hessian is $d^T \operatorname{diag}(\cosh(h + dv))d \succeq d^T d$. Its integral Taylor formula, stationarity, and the graph Poincaré inequality prove (11); coercivity on the fixed-mean slice gives existence. Exact shifts dv leave all cycle sums of h unchanged. For a cycle of q edges and circulation H, every minimizing edge value is H/q and the energy is $q[\cosh(H/q) - 1]$.

The distinction between these realizations matters. Equation (5) constrains the content coordinate $u = \sinh t$; (11) constrains logarithmic cycle sums. Both use J, with different physical constraints. A single aggregate $\cosh(\alpha \cdot t) - 1$, $\alpha \neq 0$, would instead have the rank-one log-affine Hessian $\cosh(\alpha \cdot t)\alpha\alpha^T$ [11]. Multiple responsive modes arise from the network of comparisons and its incidence, not from renaming the coordinates of one aggregate.

4. A coupled matter–field realization

A field changes the cost of moving matter between neighboring sites. If that kinetic cost depends on the field, matter also changes the field's stationary equation. Both effects follow from one functional. The finite construction below extends the reciprocal graph energy in [4]; its state and time identifications are stated explicitly.

Self-consistent wavefunction–potential coupling also occurs in the Schrödinger–Newton equation, whose potential is sourced by the instantaneous probability density [12]. Here the kinetic form depends on the field through the Hessian of $\mathcal{A}$. Its variation adds a covariant-coherence contribution to the field equation. The explicit equal-density comparison in Section 4.4 isolates that contribution within the finite model. This comparison concerns the information entering the potential; the neutral fixed-endpoint source below is not a Schrödinger–Newton self-gravity source.

4.1. The common functional and its physical inputs

Let $\mathcal{G} = (V, E)$ be a finite connected simple graph with $N \geq 2$ vertices and unit edge weights. Give each edge an arbitrary orientation $e = (i, j)$ and set $b_e = \mathbf{e}_i - \mathbf{e}_j$, $d_e h = b_e^T h$, and $\operatorname{div} q = \sum_e b_e q_e$. The explicit example will be the periodic cube $C_3 \square C_3 \square C_3$, with vertices $(\mathbb{Z}/3\mathbb{Z})^3$: two vertices are adjacent when they differ in exactly one coordinate. It has 27 vertices, six neighbors per site, and 81 unoriented edges.

The matter variable is $\psi \in \mathbb{C}^N$ with $\sum_i |\psi_i|^2 = 1$. Its probability reading is $p_i = |\psi_i|^2$, under the record conditions of Section 5.4. A fixed unit endpoint at $a \in V$ gives the neutral source $\rho_i = \delta_{ia} - p_i$. The real potential h has zero mean. Define

$$\mathcal{A}(h) = 2 \sum_e J(e^{d_e h}) = 2 \sum_e [\cosh(d_e h) - 1], \tag{12}$$

$$K_1(\psi, h) = \sum_{\{i,j\}} \cosh(h_i - h_j) |\psi_i - \psi_j|^2. \tag{13}$$

The normalization in (12) makes

$$K_1(\psi, h) = \frac{1}{2} \left(D^2\mathcal{A}(h)[\Re\psi, \Re\psi] + D^2\mathcal{A}(h)[\Im\psi, \Im\psi] \right). \tag{14}$$

Indeed $D^2\mathcal{A}(h)[v, v] = 2 \sum_e \cosh(d_e h)(d_e v)^2$. Thus the matter kinetic form is the complexified half-Hessian of the same field cost. Assigning this form to physical matter, choosing the fixed-endpoint source, and choosing the ordinary complex state metric are the physical inputs of this finite realization.

An explicit gauge-covariant extension uses static link transports $U_{ij} \in \mathbb{C}$, $|U_{ij}| = 1$, $U_{ji} = \overline{U_{ij}}$. Put

$$w_e = |\psi_i - U_{ij}\psi_j|^2, \qquad c_e = 2 - w_e, \tag{15}$$

$$K_U(\psi, h) = \sum_e \cosh(d_e h) w_e,$$

$$\mathcal{F}_U(\psi, h) = K_U(\psi, h) + \rho(\psi)^T h - \mathcal{A}(h). \tag{16}$$

Every unoriented edge is counted once. At $U = 1$, (14) is exact; the nontrivial-link expression is the stated extension. The functional is invariant under time-independent transformations $\psi_i \mapsto e^{i\alpha_i}\psi_i$, $U_{ij} \mapsto e^{i(\alpha_i - \alpha_j)} U_{ij}$, with h unchanged.

4.2. Why the kinetic response enters the field equation

For one edge with difference x, bond weight w, and conjugate source r, the field-dependent terms reduce to

$$\mathcal{F}(x) = w \cosh x + rx - 2(\cosh x - 1), \qquad \mathcal{F}'(x) = r - (2 - w) \sinh x.$$

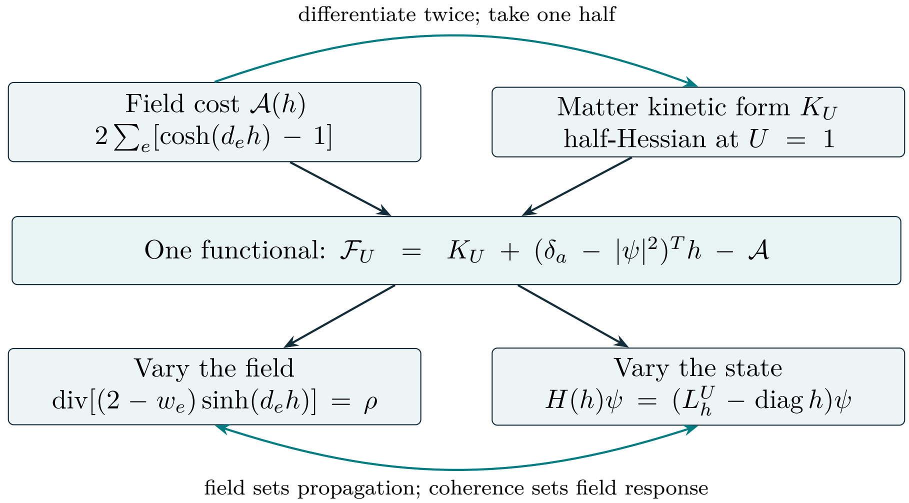

Figure 5: Bidirectional coupling from one functional. The factor $2 - w_e$ is fixed by differentiating both the field energy and its matter kinetic form. The state derivative supplies an operator; the coherent-time identification in Section 4.5 turns that operator into dynamics.

For $w = r = 1$, the stationary drop is $x = \operatorname{arsinh} 1$. Varying only the source and field-cost terms would give $x = \operatorname{arsinh}(1/2)$; at that value the full derivative is $1/2$. The omitted term changes the stationary point.

Proposition 4 (Joint variation)**.** *For* (16)*, a stationary mean-zero field obeys*

$$\boxed{\operatorname{div}[(2 - w_e)\sinh(d_e h)] = \rho.} \tag{17}$$

At fixed h, the state differential along any tangent variation η of the normalized sphere is

$$D_\psi \mathcal{F}_U[\eta] = 2\Re\langle \eta, H(h)\psi\rangle, \qquad H(h) = L_h^U - \operatorname{diag} h, \tag{18}$$

where the inner product is conjugate-linear in its first argument and

$$(L_h^U \psi)_i = \sum_{j\sim i} \cosh(h_i - h_j)(\psi_i - U_{ij}\psi_j).$$

Proof. The field derivative is

$$D_h \mathcal{F}_U[v] = \rho^T v + \sum_e (w_e - 2)\sinh(d_e h)\, d_e v.$$

Its gradient has zero sum because $\sum_i \rho_i = 0$ and every b_e has zero sum. Vanishing on mean-zero variations therefore makes the whole gradient zero, proving (17). Hermiticity of L_h^U and $K_U = \langle \psi, L_h^U \psi\rangle$ give the kinetic part of (18); differentiating $-\sum_i |\psi_i|^2 h_i$ gives its potential part. □

The additional field response is $\sum_e b_e w_e \sinh(d_e h)$. At $U = 1$ it is one half of the third derivative of $\mathcal{A}$, paired with the real and imaginary matter amplitudes. Once the kinetic assignment (14) is made, its coefficient is fixed. The positive endpoint and normalized negative source remain one unit each.

4.3. A sharp connectivity criterion for the coupled field

An edge can have $w_e = 2$, so positivity of every c_e cannot be assumed. The decisive question is whether another path remains when one bond loses its response. An edge whose removal disconnects a graph is called a bridge.

Theorem 5 (Global field solvability and its exact graph criterion)**.** *Let $\mathcal{G}$ be a finite connected simple graph with $N \geq 2$ vertices and unit edge weights. The following are equivalent:*

1. *$\mathcal{G}$ has no bridge.*
2. *For every normalized $\psi \in \mathbb{C}^N$, every source vertex a, and every static unit-modulus link configuration U, (17) has a unique mean-zero solution.*

When these conditions hold, put

$$\gamma_{\mathcal{G}} = \frac{1}{2} \min_{e \in E} \lambda_2(L_{\mathcal{G}-e}) > 0, \tag{19}$$

where λ_2 is the first nonzero Laplacian eigenvalue of the connected edge-deleted graph. The solution $h_{\psi,U}$ is the unique maximizer of $\mathcal{F}_U(\psi, \cdot)$ on mean-zero fields and depends smoothly on ψ and U. On that space,

$$M := -D_h^2 \mathcal{F}_U = \sum_e c_e \cosh(d_e h) b_e b_e^T \succeq \gamma_{\mathcal{G}} I, \qquad \|h_{\psi,U}\|_2 \leq \frac{\sqrt{2}}{\gamma_{\mathcal{G}}}. \tag{20}$$

Proof. Normalization gives $w_e \leq 2(|\psi_i|^2 + |\psi_j|^2) \leq 2$, hence $c_e \geq 0$. For distinct edges e, e', their Hermitian bond forms have sum with largest eigenvalue at most three. For disjoint edges the nonzero eigenvalues are two and two. For adjacent edges, rephasing the three vertices removes the two link phases, leaving the three-site path Laplacian with eigenvalues $0, 1, 3$. Thus $w_e + w_{e'} \leq 3$: at most one edge has $w_e > 3/2$, and every other edge has $c_e \geq 1/2$.

Suppose $\mathcal{G}$ has no bridge. Delete the exceptional edge e_0, or any edge if there is none. The remaining graph is connected. On mean-zero fields,

$$L_c := \sum_e c_e b_e b_e^T \succeq \tfrac{1}{2} L_{\mathcal{G}-e_0} \succeq \gamma_{\mathcal{G}} I. \tag{21}$$

Since $\cosh(d_e h) \geq 1$, this proves the Hessian bound. Taylor's formula at $h = 0$ gives

$$\mathcal{F}_U(\psi, h) \leq K_U(\psi, 0) + \rho^T h - \tfrac{1}{2} \gamma_{\mathcal{G}} \|h\|_2^2.$$

The functional tends to minus infinity as $\|h\|_2 \to \infty$. Strict concavity gives its unique maximizer and hence the field solution. The invertible restricted Hessian and the implicit-function theorem give smooth dependence; uniqueness makes local solution maps agree globally.

Pair the field equation with h. Since $x \sinh x \geq x^2$,

$$\rho^T h = \sum_e c_e (d_e h) \sinh(d_e h) \geq \gamma_{\mathcal{G}} \|h\|_2^2.$$

Consequently $\|h\|_2 \leq \|\rho\|_2 / \gamma_{\mathcal{G}}$. The bound $\|\rho\|_2^2 = 1 - 2p_a + \sum_i p_i^2 \leq 2$ proves (20).

Conversely, let $e = (i, j)$ be a bridge. For any fixed U, choose $\psi_i = 1/\sqrt{2}$, $\psi_j = -\overline{U_{ij}}/\sqrt{2}$, and every other amplitude zero. Then $w_e = 2$ and $c_e = 0$. Each component of $\mathcal{G} - e$ contains probability $1/2$. The component containing a has total source $1/2$. Summing (17) over that component cancels all internal fluxes, while its sole boundary edge has zero conductance. This gives $0 = 1/2$, so no solution exists. The obstruction holds for every fixed link configuration and source vertex. □

Alternate paths are the exact protection against a saturated bond. For the periodic cube $C_3 \square C_3 \square C_3$, the ordinary mean-zero Laplacian obeys $L \succeq 3I$: the single-cycle spectrum is $0, 3, 3$, and product spectra add. Since $\|b_e b_e^T\| = 2$, every edge deletion leaves $L_{\mathcal{G}-e} \succeq I$. Thus

$$\gamma_{\mathcal{G}} \geq \tfrac{1}{2}, \qquad M \succeq \tfrac{1}{2} I, \qquad \|h_{\psi,U}\|_2 \leq 2\sqrt{2} \quad \text{on the 27-site cube.} \tag{22}$$

The following dynamics use any bridgeless graph; the explicit phase experiment uses this cube. The field maximizes the joint functional, while its underlying cost $\mathcal{A}$ is positive and convex.

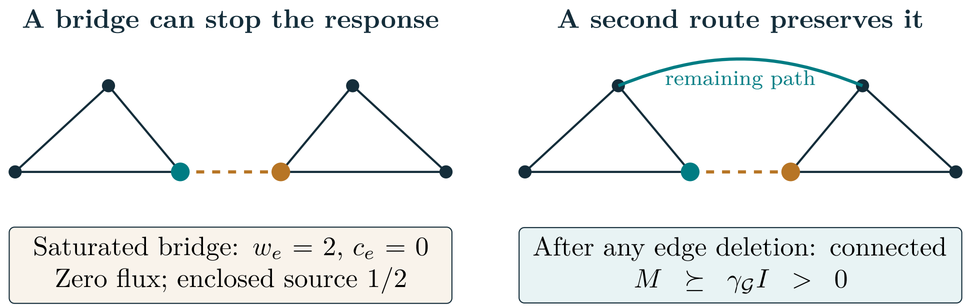

Figure 6: Why the graph criterion is sharp. Opposite endpoint amplitudes can saturate one bond. A bridge then traps a nonzero source behind zero conductance. On a graph without bridges, all remaining bonds retain enough response to give a unique field.

4.4. An exact field change at fixed probability density

Now take $\mathcal{G} = C_3 \square C_3 \square C_3$, set $U = 1$, choose $a = (0,0,0)$, and prepare

$$\psi_\theta(a) = \frac{e^{i\theta}}{\sqrt{27}}, \qquad \psi_\theta(i) = \frac{1}{\sqrt{27}} \quad (i \neq a). \tag{23}$$

Every preparation has $p_i = 1/27$ and the same source $\rho = \delta_a - \mathbf{1}/27$. Its six bonds incident on a have $w_e = 2(1-\cos\theta)/27$; all other bonds have $w_e = 0$.

Proposition 6 (Phase-sensitive field with unchanged density)**.** *Write $h_\theta = h_{\psi_\theta,1}$. For each of the six neighbors b of a,*

$$h_\theta(a) - h_\theta(b) = \delta_\theta := \operatorname{arsinh}\frac{13}{6(26+\cos\theta)}. \tag{24}$$

In fact the complete field difference is

$$h_\theta - h_0 = (\delta_\theta - \delta_0)(\delta_a - \mathbf{1}/27). \tag{25}$$

In particular $\delta_0 = \operatorname{arsinh}(13/162)$ and $\delta_\pi = \operatorname{arsinh}(13/150)$ are different although the two preparations have identical density and zero instantaneous current under the evolution below.

Proof. Coordinate permutations and independent sign reversals preserve the graph, source, and bond weights. Uniqueness makes h_θ invariant under these symmetries. The field therefore has one value v_k on each class with k nonzero coordinates, whose sizes are $(1,6,12,8)$. Let $d_k = v_k - v_{k+1}$ for $k = 0,1,2$.

Summing (17) over successive unions of classes cancels internal fluxes. The three cuts have $6, 24, 24$ crossing edges and enclosed sources $26/27, 20/27, 8/27$. Only the first cut has coefficient $c_e = 2(26+\cos\theta)/27$; both outer cuts have coefficient two. Hence

$$\sinh d_0 = \frac{13}{6(26+\cos\theta)}, \qquad \sinh d_1 = \frac{5}{324}, \qquad \sinh d_2 = \frac{1}{162}.$$

The mean-zero condition gives $v_3 = -(d_0 + 7d_1 + 19d_2)/27$. Only d_0 changes with θ, proving (25). The current in (28) is proportional to $\sin\theta$ on the six incident edges and vanishes on the others. It is zero at $\theta = 0, \pi$. □

This is a difference in phase relative to fixed links. A simultaneous gauge transformation of state and links preserves w_e and h, whereas (23) holds the links fixed. The field distinguishes coherent preparations that a density-only source equation would assign the same potential. Zero instantaneous current does not make either preparation a stationary state.

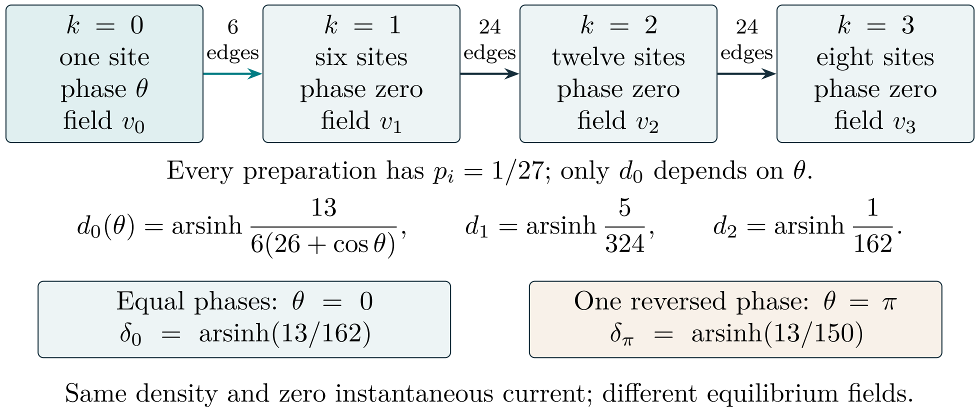

Figure 7: The exact 27-site solution, reduced by symmetry. The four boxes collect sites with the same number of nonzero coordinates relative to the source. Edges within a class carry no field difference and are omitted. The six inner bonds transmit the phase-dependent kinetic response; the outer drops remain fixed.

4.5. Conserved dynamics, current, and field response

Return to a finite connected simple graph $\mathcal{G}$ without bridges, with fixed source a and fixed static unit-modulus links U. Eliminate the unique field by defining $\mathcal{E}_U(\psi) = \max_{\mathbf{1}^T h=0} \mathcal{F}_U(\psi, h)$. The envelope identity and (18) give $D\mathcal{E}_U[\eta] = 2\Re\langle \eta, H(h_{\psi,U})\psi\rangle$. To supply a physical time law, adopt the coherent-state temporal term

$$\mathcal{S}_U = \int \left[\frac{i}{2}(\langle \psi, \dot\psi\rangle - \langle \dot\psi, \psi\rangle) - \mathcal{E}_U(\psi)\right] ds, \qquad s = t/\tau_0, \quad E_0\tau_0 = \hbar. \tag{26}$$

Here $E_0 > 0$ is the adopted energy unit; physical action and energy are $\hbar\mathcal{S}_U$ and $E_0\mathcal{E}_U$. Variation on the normalized sphere gives the equation below up to an overall phase, chosen to remove the normalization multiplier. The temporal term is an additional physical identification, separate from the finite cost and its Hessian.

Theorem 7 (Global evolution and local conservation)**.** *For fixed static U, every normalized initial state has a unique solution for all real s of*

$$i\dot\psi = (L_h^U - \operatorname{diag} h)\psi, \qquad h = h_{\psi,U}. \tag{27}$$

Its norm and $\mathcal{E}_U$ are conserved. For $U_{ij} = e^{iA_{ij}}$, the same energy gives the current

$$\begin{gathered} j_{ij} = \frac{\partial \mathcal{E}_U}{\partial A_{ij}} = 2\cosh(h_i - h_j)\Im(\overline{\psi_i} U_{ij}\psi_j), \\ \dot p_i = -\sum_{j\sim i} j_{ij}, \qquad j_{ji} = -j_{ij}. \end{gathered} \tag{28}$$

There are self-consistent stationary rays satisfying $H(h)\psi = \lambda\psi$ together with (17).

Proof. Theorem 5 makes the vector field $-iH(h_{\psi,U})\psi$ smooth. Hermiticity gives

$$\frac{d}{ds}\|\psi\|^2 = 2\Re\langle \psi, -iH\psi\rangle = 0,$$

so the vector field is tangent to the compact unit sphere. Local existence and uniqueness extend globally because a smooth vector field on a compact manifold is complete. The envelope identity gives

$$\frac{d\mathcal{E}_U}{ds} = 2\Re\langle -iH\psi, H\psi\rangle = 0.$$

At the stationary field, implicit derivatives of h drop out of the link derivative. Differentiating $|\psi_i - e^{iA_{ij}}\psi_j|^2$ gives the displayed j_{ij}. Directly expanding (27), its real diagonal terms contribute zero to $\dot{p}_i$, and each off-diagonal term contributes $-2\cosh(h_i - h_j)\Im(\overline{\psi_i}U_{ij}\psi_j)$. This proves continuity.

Finally, $\mathcal{E}_U$ attains extrema on the sphere. At each extremum its tangent differential vanishes, hence $H(h)\psi = \lambda\psi$ for real λ. Overall-phase invariance keeps h fixed along $e^{-i\lambda s}\psi$, giving a stationary ray. □

The current and propagation have the same variational origin. The scalar field is instantaneously constrained by the matter state at every time. In the preparation (23),

$$j_{ab} = -\frac{2}{27}\cosh\delta_\theta \sin\theta, \qquad \dot{p}_a = \frac{4}{9}\cosh\delta_\theta \sin\theta.$$

Thus the phase determines both the field adjustment and the initial probability transfer. The evolution is nonlinear through $h_{\psi,U}$; it is not a state-independent linear unitary propagator. Time-dependent gauge transformations would additionally require a temporal connection. A stationary multiplier is an eigenfrequency of this finite dynamics; it is not by itself a particle mass or the total energy. Indeed $\mathcal{E}_U = \lambda + h(a) - \mathcal{A}(h)$ on a normalized stationary state.

Field relaxation also enters response calculations. For a tangent state variation at fixed U, differentiating (17) gives

$$M\,\delta h = \delta\rho + \sum_e b_e\,\delta w_e \sinh(d_e h), \qquad \|M^{-1}\| \le \gamma_{\mathcal{G}}^{-1} \tag{29}$$

on mean-zero fields; the bound is two on the 27-site cube. In local real coordinates x on the normalized sphere, the eliminated energy therefore has the exact Hessian

$$(\mathcal{E}_U)_{xx} = (\mathcal{F}_U)_{xx} + (\mathcal{F}_U)_{xh} M^{-1} (\mathcal{F}_U)_{hx}. \tag{30}$$

Here h is represented in a fixed basis of the mean-zero space and all derivatives are evaluated at its stationary value. The second term is positive semidefinite: $h_x = M^{-1}(\mathcal{F}_U)_{hx}$ follows by differentiating $(\mathcal{F}_U)_h = 0$, and substitution proves (30). The plus sign reflects maximization over h. The state Hessian with h fixed omits this response. As in Theorem 3, the response operator is obtained by differentiating the actual constrained variational problem.

For small field differences, (17) has leading operator $L_c h = \rho$, with $c_e = 2 - w_e$ held at the chosen state. Although the field correction to L_h^U begins at second order through $\cosh(d_e h)$, its kinetic backreaction in the field equation begins at first order through $w_e \sinh(d_e h)$. Weak field alone therefore does not justify a density-only field equation; dropping this term additionally requires small covariant bond differences. The geometric gravitational identification of this finite potential and its extension to physical charged fields remain the construction targets in Section 8.

4.6. A unique coherent ground state

For trivial links, the coupled equilibrium has a stronger structure than existence of stationary rays. Its energy is convex in probability density, even though its evolution is nonlinear in the complex amplitudes.

Theorem 8 (Unique positive ground state and orbital stability)**.** *Let $\mathcal{G}$ be a finite connected simple graph without bridges, fix a, and take $U = 1$. There is exactly one strictly positive real normalized vector r satisfying*

$$(L^1_{h_*} - \operatorname{diag} h_*)r = \lambda_* r, \qquad h_* = h_{r,1}. \tag{31}$$

The global minimizers of $\mathcal{E}_1$ on the complex unit sphere are precisely $e^{i\alpha}r$. This phase orbit is Lyapunov stable under (27). Every graph automorphism fixing a preserves r and h_*.

Proof. For p in the probability simplex and fixed mean-zero h, define

$$\Phi_h(p) = \sum_{\{i,j\}} \cosh(h_i - h_j)(p_i + p_j - 2\sqrt{p_i p_j}) - p^T h + h(a) - \mathcal{A}(h).$$

The geometric mean is concave on the nonnegative quadrant, so each Φ_h is convex. Therefore

$$\varepsilon(p) := \mathcal{E}_1(\sqrt{p}) = \max_h \Phi_h(p)$$

is convex on the simplex. For interior p and a tangent vector v, direct differentiation gives

$$D^2\Phi_h(p)[v,v] = \frac{1}{2} \sum_{\{i,j\}} \cosh(h_i - h_j)\sqrt{p_i p_j} \left(\frac{v_i}{p_i} - \frac{v_j}{p_j} \right)^2. \tag{32}$$

It is positive for every nonzero v with $\sum_i v_i = 0$: equality on a connected graph makes v_i/p_i constant, and the zero sum makes that constant zero. Taking the maximizing field at an interior point of any segment proves strict convexity of ε in the interior. Equivalently, field relaxation adds the positive semidefinite term in (30) to (32).

The smooth energy $\mathcal{E}_1$ has a minimum on the unit sphere. Replacing ψ by $|\psi|$ preserves the source and reduces every bond difference, since $|\psi_i - \psi_j| \geq ||\psi_i| - |\psi_j||$. This inequality holds at every h, and hence after maximization. There is a nonnegative real minimizer r. Stationarity on the complex sphere gives (31). If $r_i = 0$, its ith equation becomes

$$0 = -\sum_{j\sim i} \cosh(h_{*,i} - h_{*,j}) r_j.$$

Every neighbor must also vanish. Connectivity would force $r = 0$, a contradiction. Thus $r > 0$ and its density lies in the simplex interior, where strict convexity gives uniqueness.

For any other positive stationary vector, the envelope identity in density coordinates gives

$$D\varepsilon(p)[v] = \sum_i \frac{(H(h_{\sqrt{p},1})\sqrt{p})_i}{\sqrt{p_i}} v_i = \lambda \sum_i v_i = 0.$$

Convexity makes it a global minimum, so it is the same r. Any complex minimizer has density r_i^2. At the maximizing field h_*, equality in the bond inequality then forces equal phases on every edge; connectivity makes the phase global. This proves the asserted minimizing orbit.

For stability, write $\mathcal{O} = \{e^{i\alpha} r\}$. For any $\epsilon > 0$ with nonempty complement, the compact set of normalized states at distance at least ϵ from $\mathcal{O}$ has energy at least $\mathcal{E}_1(r) + \Delta_\epsilon$, for some $\Delta_\epsilon > 0$. Continuity gives a neighborhood of $\mathcal{O}$ below that level, and energy conservation prevents a trajectory from leaving the ϵ-neighborhood. Finally, a graph automorphism fixing a preserves the functional. Uniqueness of the positive minimizer and of its field gives the symmetry statement. □

The equilibrium is selected by the same field-dependent kinetic energy that governs propagation. Stability means remaining close to its phase orbit; the conservative dynamics need not approach it. Excited stationary rays may also exist. On the 27-site cube, source-fixing symmetries make r and h_* constant on the four classes of Figure 7, reducing the equilibrium equations to four amplitudes and three independent field drops.

Proposition 9 (Ground-state transform and reversible transport)**.** *At the equilibrium of Theorem 8, set $H_* = L^1_{h_*} - \operatorname{diag} h_*$ and $k_{ij} = \cosh(h_{*,i} - h_{*,j})$. For every $z \in \mathbb{C}^N$,*

$$\langle z, (H_* - \lambda_*) z \rangle = \sum_{\{i,j\}} k_{ij} r_i r_j \left| \frac{z_i}{r_i} - \frac{z_j}{r_j} \right|^2. \tag{33}$$

Thus λ_* is the simple lowest eigenvalue of H_*. Define the continuous-time Markov generator acting on functions by

$$Q_{ij} = k_{ij}\frac{r_j}{r_i} \quad (i \sim j), \qquad Q_{ii} = -\sum_{j\sim i} Q_{ij}, \qquad Q_{ij} = 0 \quad (i \neq j,\ i \not\sim j). \tag{34}$$

It is reversible with stationary distribution $p_i^* = r_i^2$. With $R = \operatorname{diag} r$,

$$R^{-1}(H_* - \lambda_*)R = -Q, \qquad e^{-\tau(H_*-\lambda_*)} = Re^{\tau Q}R^{-1} \quad (\tau \geq 0). \tag{35}$$

Let $\Delta_* > 0$ be the gap from λ_* to the next eigenvalue of H_*. Every normalized complex state satisfies the global energy barrier

$$\mathcal{E}_1(\psi) - \mathcal{E}_1(r) \geq \Delta_*(1 - |\langle r, \psi\rangle|^2) \geq \frac{\Delta_*}{2}\operatorname{dist}(\psi, \mathcal{O})^2, \qquad \mathcal{O} = \{e^{i\alpha}r\}. \tag{36}$$

Proof. The eigenvalue equation gives $(H_{*,ii} - \lambda_*)r_i = \sum_{j\sim i} k_{ij}r_j$. Expanding the right side of (33) gives exactly these diagonal coefficients and the off-diagonal terms $-2k_{ij}\Re(\overline{z}_i z_j)$. Its nullspace consists of z_i/r_i constant on the connected graph, hence is spanned by r. The similarity is entrywise. The rates are positive on edges, each row sums to zero, and

$$p_i^* Q_{ij} = k_{ij}r_ir_j = p_j^* Q_{ji}.$$

These are the detailed-balance equations; they imply stationarity. The exponential identity follows from similarity.

For the energy barrier, evaluate the maximizing functional at h_*:

$$\mathcal{E}_1(\psi) - \mathcal{E}_1(r) \geq \mathcal{F}_1(\psi, h_*) - \mathcal{F}_1(r, h_*) = \langle \psi, (H_* - \lambda_*)\psi\rangle.$$

Decompose ψ into its component along r and its orthogonal complement. The spectral gap gives the first inequality in (36). Finally $\operatorname{dist}(\psi, \mathcal{O})^2 = 2(1 - |\langle r, \psi\rangle|)$ and $1 - c^2 \geq 1 - c$ for $0 \leq c \leq 1$ give the second. □

The same positive bond conductance controls the equilibrium spectrum, reversible probability flow, and nonlinear stability. Conservation turns (36) into an explicit all-time estimate:

$$\operatorname{dist}(\psi(s), \mathcal{O}) \leq \sqrt{\frac{2[\mathcal{E}_1(\psi(0)) - \mathcal{E}_1(r)]}{\Delta_*}} \qquad (s \in \mathbb{R}).$$

Equation (35) concerns imaginary time at the fixed equilibrium field. The real-time coupled dynamics remains (27), with its changing self-consistent field.

5. Geometry, quantum records, and propagation

5.1. From cycle closure to the Newtonian field

An antisymmetric edge field has zero sum around every cycle if and only if it is an exact potential difference $d\Phi$. To see this, define $\Phi(v)$ by summing the field along a path from a root to v. Cycle closure makes the sum independent of the path. The converse follows by telescoping. This published ledger-to-potential result [3] supplies the precise integrability premise for a scalar gravitational field; vertex conservation alone would not supply it.

Choose positive mesh weights w_e, vertex volumes ν_v, a mass density ρ_v, fixed Dirichlet boundary data, and a potential unit $\Phi_* > 0$. The reciprocal-cost realization

$$\mathcal{E}(\Phi) = \frac{\Phi_*^2}{4\pi G}\sum_e w_e J\left(e^{(d\Phi)_e/\Phi_*}\right) + \sum_v \nu_v\rho_v\Phi_v \tag{37}$$

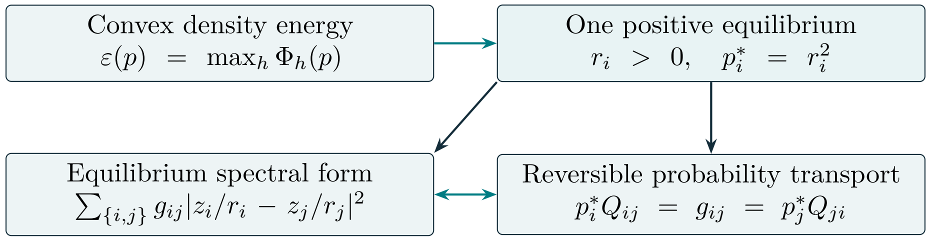

$g_{ij} = \cosh(h_{*,i} - h_{*,j}) r_i r_j$
One equilibrium conductance, two exact mathematical readings.

Figure 8: Coherent equilibrium and probability transport. Density convexity selects a unique positive state. Its ground-state transform gives a reversible Markov flow with that state's Born distribution. The transform is exact for the frozen equilibrium operator; nonlinear real-time stability follows separately from conserved energy.

has, for $|(d\Phi)_e| \ll \Phi_*$, the quadratic field term $\sum_e w_e (d\Phi)_e^2/(8\pi G)$. Interior variation gives

$$\frac{\Phi_*}{4\pi G} d^T \operatorname{diag}(w_e) \sinh(d\Phi/\Phi_*) + \operatorname{diag}(\nu_v)\rho = 0.$$

Linearization therefore yields

$$\Delta_h \Phi = 4\pi G \rho, \qquad \Delta_h = -\operatorname{diag}(\nu_v)^{-1} d^T \operatorname{diag}(w_e) d. \tag{38}$$

With consistent mesh weights and refinement convergence this becomes $\Delta\Phi = 4\pi G\rho$, the Newton–Poisson limit developed in the published classical-gravity construction [6]. The factor $1/2$ in the expansion of J fixes the factor in the Dirichlet action. The dimensional normalization uses the measured G; its absolute value is not determined by this limit.

5.2. The geometric action

On a piecewise-flat geometry with lengths q, hinge area $\mathcal{A}_h(q)$, and deficit $\delta_h(q)$, the geometric action is

$$S_R(q) = \sum_h \mathcal{A}_h(q) \delta_h(q). \tag{39}$$

This is the Regge action [13]; its weak-field relation to continuum gravity has a long-established lattice formulation [14]. Identifying the contents in (5) with deficits is an additional geometric premise of the RS realization [10]. With its specified midpoint embedding on a periodic four-dimensional triangulation, the transverse-traceless quadratic coefficient is one half of the Einstein–Hilbert coefficient before overall normalization. The exact metric block also supplies a direct count of physical modes [10, 15].

The positive response W and the signed action S_R are different functions. A positive cost can control a stable response while a constrained gravitational action has gauge directions and an indefinite unreduced quadratic form. Relating their variational roles is part of the common dynamical construction, addressed in Section 8.

Proposition 10 (Two physical metric modes)**.** *Let $p \in \mathbb{C}^4$ have at least one nonzero component modulo 2π. Write*

$$f_\mu = e^{ip_\mu} - 1, \qquad \widetilde{f}_\mu = 1 - e^{-ip_\mu}, \qquad L(p) = 4\sum_{\mu=1}^{4} \sin^2(p_\mu/2).$$

Define the 4×10 matrix $C(p)$ by its four diagonal and six off-diagonal columns,

$$C_{(\mu)} = f_\mu e_\mu, \qquad C_{(\mu\nu)} = \widetilde{f}_\nu e_\mu + \widetilde{f}_\mu e_\nu \quad (\mu < \nu),$$

and set $B_4 = I_4 - \frac{1}{2}\mathbf{1}\mathbf{1}^T$, $V = \operatorname{diag}(B_4/2, I_6)$. *For the metric block*

$$E(p) = L(p)V - C(-p)^T C(p), \qquad G(p) = V^{-1}C(-p)^T, \tag{40}$$

the gauge subspace $\operatorname{im} G$ *has dimension four and lies in* $\ker E$. *Off the characteristic branch* $L = 0$, *it is all of* $\ker E$. *On* $L = 0$, $\dim\ker E = 6$ *and*

$$\dim\big(\ker E/\operatorname{im} G\big) = 2.$$

Proof. Since $B_4^2 = I_4$, direct multiplication gives

$$C(p)V^{-1}C(-p)^T = L(p)I_4. \tag{41}$$

Each diagonal entry is $f_\mu(p)f_\mu(-p)+\sum_{\nu\neq\mu}\widetilde{f}_\nu(p)\widetilde{f}_\nu(-p) = L(p)$; the off-diagonal entries cancel. To check rank even on $L = 0$, suppose $y^T C(p) = 0$. Diagonal columns imply $y_\mu = 0$ whenever $f_\mu \neq 0$. Choose one such index. For each remaining ν, the $(\mu\nu)$ column then implies $y_\nu \widetilde{f}_\mu = 0$, so $y = 0$. Thus $C(p)$ and $C(-p)$ both have rank four. Equation (41) gives $EG = 0$. If $L \neq 0$, $Eh = 0$ implies $h = L^{-1}GC(p)h$, proving $\ker E = \operatorname{im} G$. If $L = 0$, the injectivity of $C(-p)^T$ gives $\operatorname{rank} E = \operatorname{rank} C(p) = 4$, so its nullity is six. Quotienting by the four independent gauge vectors leaves two modes. □

The calculation counts modes of the displayed geometric metric block; the reduction from edge lengths to this block is supplied by the specified triangulation [10, 15]. Complex continuation permits a nonzero characteristic branch. For real Euclidean momentum, L vanishes only at zero modulo 2π.

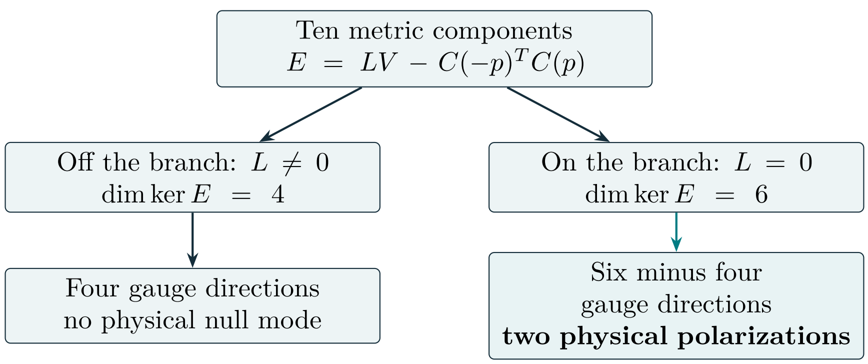

Figure 9: The two-mode count at nonzero momentum. The gauge rank remains four on the characteristic branch; two additional null directions become physical after quotienting. The count does not identify every off-shell tensor component as a polarization.

5.3. An exact cost-to-state construction

The published recognition-operator construction supplies an explicit map from reciprocal cost to normalized amplitudes [5]. Let S be a nonzero subspace of a finite-dimensional complex Hilbert space, $s \in S$ a unit vector, and $T : \mathbb{R}^N \to S^\perp$ a real-linear isometric embedding. For $\eta \in \mathbb{R}^N$, set

$$\chi_a = 2\sinh(\eta_a/2), \qquad \Psi(\eta) = \sqrt{1 - \|\chi\|^2}\, s + T\chi, \qquad \|\chi\| < 1. \tag{42}$$

Orthogonality gives $\|\Psi\| = 1$, while the half-angle identity gives

$$\frac{1}{2}\|\Pi_{S^\perp}\Psi\|^2 = \frac{1}{2}\sum_a 4\sinh^2(\eta_a/2) = \sum_a J(e^{\eta_a}). \tag{43}$$

For an outcome-register basis adapted to $S \oplus S^{\perp}$, with a preparation domain of at least three registers satisfying Section 5.4, the probability in $S^{\perp}$ is $2\sum_a J(e^{\eta_a})$. The construction requires total cost below 1/2 and a physical preparation that selects the map.

The same published construction gives an exact discrete-to-continuous evolution. For the unitary cyclic shift P on $\mathbb{C}^8$, choose $\mathcal{V} = \ker(P^4 + I)$, a time step $\tau_0 > 0$, and the principal logarithm. Then

$$H = \frac{i\hbar}{\tau_0} \operatorname{Log}(P|_{\mathcal{V}}), \qquad U(t) = e^{-itH/\hbar}, \qquad U(n\tau_0) = P^n|_{\mathcal{V}}. \tag{44}$$

The Fourier eigenphases are $\pm\pi/4, \pm 3\pi/4$. Hence H is self-adjoint, with energy set $\{\pm 1, \pm 3\}\pi\hbar/(4\tau_0)$, and differentiating U gives $i\hbar\partial_t \Psi = H\Psi$. The Hilbert carrier, antiperiodic sector, time scale, and logarithm branch are explicit inputs.

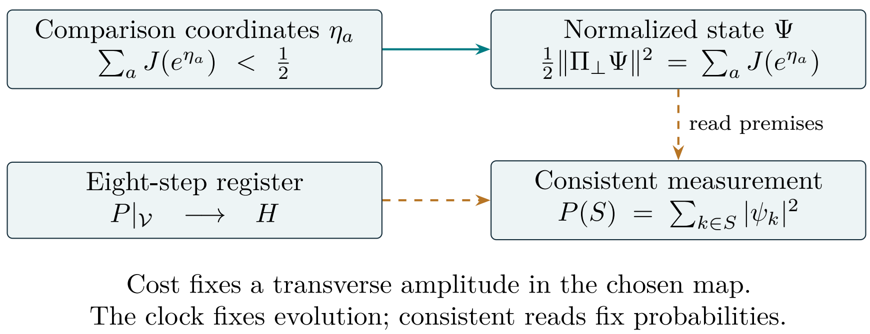

Figure 10: Three distinct pieces of the quantum construction and their connections. The state map is exact on its stated domain, the Hamiltonian interpolates the selected shift exactly, and the measurement theorem supplies the read rule.

5.4. Why normalized records give Born probabilities

For a normalized complex state $\psi \in \mathbb{C}^N$, $N \geq 3$, suppose reads are nonnegative, additive on disjoint registers, sum to one, vanish at zero amplitude, and give equal single-register reads whenever magnitudes agree, including across different preparations. These operational conditions fix the probability rule [16].

Proposition 11 (Read uniqueness)**.** *Under these conditions, $P_\psi(S) = \sum_{k\in S} |\psi_k|^2$.*

Proof. The common magnitude response defines $g(x)$ for squared amplitude $x \in [0, 1]$. Compare the normalized three-register states with squared magnitudes $(x, y, 1 - x - y)$ and $(x + y, 0, 1 - x - y)$. Total-read normalization and equality of the last reads imply

$$g(x + y) = g(x) + g(y), \qquad x, y \geq 0, \quad x + y \leq 1.$$

Also $g(0) = 0$, $g(1) = 1$, and positivity makes g monotone. Additivity gives $g(p/q) = p/q$ on rationals in the interval. Approximating each real number from above and below by rationals forces $g(x) = x$. Disjoint additivity then gives the result for every S. □

The proof needs neither an independent continuity axiom for the reads nor a separately calibrated angular probability. Combined with (43), it gives an exact probability reading of reciprocal cost for the constructed preparations. Shared single-register response and disjoint additivity have separate operational roles. They can be isolated directly. With $p_k = |\psi_k|^2$, the alternative read

$$P_\psi(S) = \frac{\sum_{k\in S} p_k^2}{\sum_j p_j^2}$$

remains nonnegative, normalized, silent at zero, and additive. But the first-register read is $1/2$ for $p = (1/2, 1/2, 0)$ and $2/3$ for $p = (1/2, 1/4, 1/4)$, despite the same first magnitude. Conversely, $P_\psi(S) = (\sum_{k\in S} p_k)^2$ preserves the shared singleton response and total read one but violates disjoint additivity: two registers of weight $1/2$ give a combined read of one and singleton reads summing to $1/2$. These witnesses isolate the operational content of the two assumptions.

5.5. An exact relation between gravity and light

Choose dimensionless spatial momenta $k_j \in [-\pi, \pi]$ and

$$Q(\mathbf{k}) = \sum_{j=1}^{3} \sin^2(k_j/2).$$

For the common spatial operator, continuous photon evolution gives $\omega_\gamma = 2\sqrt{Q}$. The specified imaginary-frequency continuation of the gravitational metric gives $4\sinh^2(\omega_g/2) = 4Q$ [15]. A common clock fixes the comparison between them.

Proposition 12 (Equal-momentum propagation)**.** *On these branches at nonzero momentum,*

$$\omega_g = 2\,\mathrm{arsinh}(\omega_\gamma/2), \qquad \mathbf{v}_g = \frac{\mathbf{v}_\gamma}{\sqrt{1+\omega_\gamma^2/4}}, \quad \mathbf{v}_a = \nabla_{\mathbf{k}}\omega_a. \tag{45}$$

Proof. Eliminate Q to obtain the frequency relation. Differentiate using $\frac{d}{dx}[2\,\mathrm{arsinh}(x/2)] = (1 + x^2/4)^{-1/2}$. $\square$

Both gravitational polarizations have the same branch. Where the group velocity is nonzero, their rays are parallel to photon rays at equal momentum. Both branches approach the same speed at long wavelength. The different finite-wavelength speeds are an additional prediction of the specified time readings.

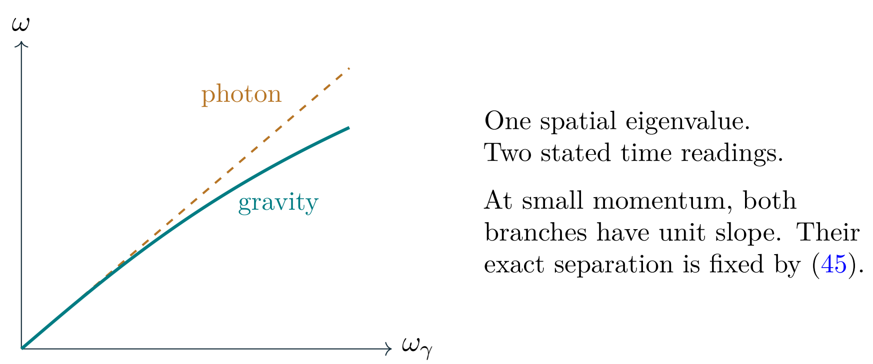

Figure 11: The exact gravitational frequency as a function of the photon frequency at the same momentum. Units are the shared lattice units. The plot is the analytic relation, not an observational fit.

6. Matter and interactions from a common response

An interaction strength measures how a state responds to a source. A mass measures how a charged excitation propagates in time. Section 4 supplies one concrete functional whose state variation, field variation, and link derivative determine coupled dynamics and a conserved current. A quantum generating function on the physical charged carrier must further determine the source response and long-time propagation together.

For a finite measure space and smooth action S_t, define

$$Z_j(t) = \int O_j \, e^{-S_t} \, d\mu, \qquad G_j = Z_j/Z_0, \qquad O_0 = 1. \tag{46}$$

The insertion O_j creates and removes a specified charge. Assume it is independent of t, the measure is fixed, differentiation twice under the integral is valid, and Z_j, Z_0 do not vanish locally. Inserted expectations are the corresponding normalized integrals. They may be complex; covariance below is the algebraic second cumulant without complex conjugation.

Proposition 13 (Shared-action response identity)**.** *Writing $H_j = -\partial_t^2 \log Z_j$, one has*

$$H_j = \langle S_t'' \rangle_j - \operatorname{Cov}_j(S_t', S_t'), \qquad -\partial_t^2 \log G_j = H_j - H_0. \tag{47}$$

If a real dimensionless decay energy $\epsilon_j = -\lim_{N\to\infty} N^{-1} \log G_j(N,t)$ exists, with N the number of time steps, and two source derivatives commute with this limit, then

$$\epsilon_j'' = \lim_{N\to\infty} \frac{H_j(N,t) - H_0(N,t)}{N}, \qquad E_j = \frac{\hbar}{\tau_0}\epsilon_j.$$

Here E_j is the physical energy and τ_0 is the shared time step, held fixed under source variation.

Proof. Differentiation gives $Z_j'/Z_j = -\langle S_t' \rangle_j$ and $Z_j''/Z_j = \langle (S_t')^2 - S_t'' \rangle_j$. Subtracting $(Z_j'/Z_j)^2$ proves the first identity. The second follows from $\log G_j = \log Z_j - \log Z_0$ on a local logarithm branch. The last statement follows under the stated limit hypothesis. □

This familiar differentiation identity is useful here because it states an exact unification condition: the source response used to determine a coupling and the response of a particle's energy must come from the same action and measure. Changing the action separately for different sectors changes the predicted responses and removes this common-source comparison.

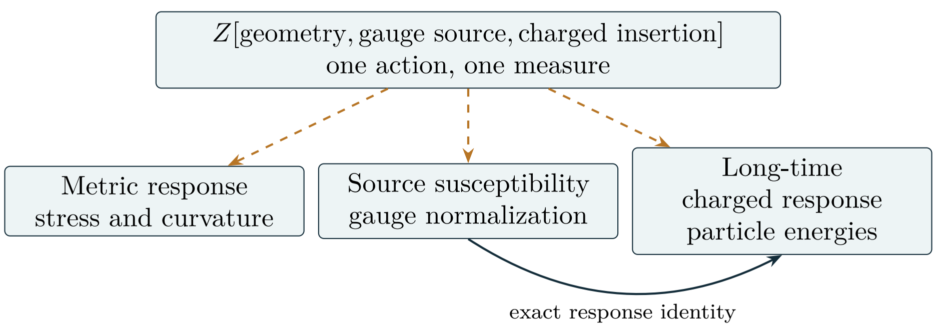

Figure 12: The common dynamical object to be realized. The charged-to-source relation is the identity in Proposition 13. A physical action must also supply the geometry and particle identifications, the time limit, and the normalization.

The compact electromagnetic construction fixes a concrete setting for studying the gauge response [17]. To include a charged insertion, consider the following finite realization. Let a_e be edge phases, ϑ vertex phases, and integer cellular boundary matrices $B \in \mathbb{Z}^{V\times E}$, $C \in \mathbb{Z}^{E\times P}$ with $BC = 0$, acting on real lifts of the phases. For $\beta, \kappa > 0$ and $\theta = a + B^T\vartheta$, set

$$S = \beta \sum_p [1 - \cos(C^T a)_p] + \kappa \sum_e (1 - \cos\theta_e).$$

Under $\vartheta \mapsto \vartheta + \chi$, $a \mapsto a - B^T\chi$, both θ and $C^T a$ are unchanged because $C^T B^T = 0$. The action is exactly gauge invariant. A corresponding charged insertion is $O_j = \exp(ij^T\theta)$, $j \in \mathbb{Z}^E$. With B the source-minus-target incidence, its endpoint charges are Bj. Holding this insertion fixed while varying an action coefficient gives the setting of Proposition 13.

Proposition 14 (The gauge source is the conserved matter current)**.** *For the compact action above, let $\jmath_e = \sin\theta_e$, with sine acting componentwise. The current is gauge invariant, and*

$$\nabla_a S = \beta C \sin(C^T a) + \kappa \jmath, \qquad \nabla_\vartheta S = \kappa B \jmath. \tag{48}$$

Matter stationarity gives $B\jmath = 0$. Joint stationarity also gives the sourced gauge equation $\beta C \sin(C^T a) + \kappa \jmath = 0$.

Proof. Differentiate $1 - \cos x$ along real lifts of the phases. Its derivative is $\sin x$, and periodicity makes the choice of lift irrelevant. The chain rule gives both gradients. Gauge invariance of θ gives that of $\jmath$, while $\kappa > 0$ turns matter stationarity into $B\jmath = 0$. Applying B to the gauge equation gives the same identity because $BC = 0$. □

The hopping term determines both the source in the gauge equation and the conserved matter current, with its coefficient κ fixed by that action. This finite spacetime boundary identity is the compact counterpart of the common-current construction in (28).

This finite realization specifies a scalar charged field; its physical history weights and the meanings of β, κ still require selection. The electric reference and long-time photon normalization determine which susceptibility is the measured coupling. Extending the construction to alternating fermion sources and nonabelian gauge sectors requires their representation content and interactions to be selected.

6.1. Spectral information and charged-lepton masses

For a Hermitian three-state coupling C with zero diagonal, define the oriented entries $u = C_{12}$, $v = C_{23}$, $w = C_{31}$ and $\mu_n = \operatorname{tr} C^n$ for $n \geq 0$. Then

$$\mu_2 = 2(|u|^2 + |v|^2 + |w|^2), \qquad \mu_3 = 6\Re(uvw).$$

The characteristic identity gives

$$C^3 = \frac{\mu_2}{2} C + \frac{\mu_3}{3} I, \qquad \mu_{n+3} = \frac{\mu_2}{2}\mu_{n+1} + \frac{\mu_3}{3}\mu_n. \tag{49}$$

For completeness, $\operatorname{tr} C = 0$ makes the characteristic polynomial $z^3 - (\mu_2/2)z - \mu_3/3$; Cayley–Hamilton proves (49), and taking traces after multiplying by C^n gives the recurrence. Thus two coherent returns determine the remaining spectral invariants once the three-state operator is physically identified [18]. Figure 13 shows why the second and third returns carry different information.

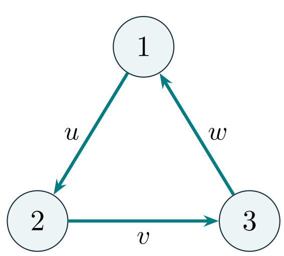

Two steps: strength
$\mu_2 = 2(|u|^2 + |v|^2 + |w|^2)$

Three steps: coherent cycle phase
$\mu_3 = 6\Re(uvw)$

Rephasing the vertices preserves the cycle product.

Figure 13: Closed returns of a Hermitian three-state coupling. Reverse entries are complex conjugates. The second return measures edge strengths; the third measures their coherent product. Together they fix the characteristic polynomial, while a physical mass interpretation additionally requires temporal propagation.

Equal-time covariance alone does not fix particle masses. For any fixed positive-definite 3×3 covariance K_0, all matrices

$$G_\epsilon(N) = K_0^{1/2} \operatorname{diag}(e^{-N\epsilon_1}, e^{-N\epsilon_2}, e^{-N\epsilon_3}) K_0^{1/2}$$

share $G_\epsilon(0) = K_0$ for any choice of positive dimensionless decay energies. Their physical energies are $E_i = (\hbar/\tau_0)\epsilon_i$. Temporal propagation supplies the missing physical information.

The published lepton construction provides a quantitative reference [19]. With its structural mass rules, an electron anchor, and external electromagnetic coupling, it gives

$$L_1 = 11 + \frac{1}{4\pi} - \alpha^2, \qquad L_2 = 6 - \frac{37}{2}\alpha, \tag{50}$$

$$m_\mu/m_e = \varphi^{L_1}, \qquad m_\tau/m_\mu = \varphi^{L_2}. \tag{51}$$

Using $\alpha^{-1} = 137.035999177$ yields

$$(m_\mu/m_e)_{\text{law}} = 206.768140397\ldots, \qquad (m_\tau/m_\mu)_{\text{law}} = 16.815597225\ldots.$$

Against 206.7682827(46) retained in [18], the first ratio is low by 0.688 parts per million, or 30.94 quoted experimental standard uncertainties. For the second ratio, the PDG 2024 inputs $m_\tau = 1776.93 \pm 0.09$ MeV and $m_\mu = 105.6583755 \pm 0.0000023$ MeV give $m_\tau/m_\mu = 16.817691845 \pm 0.000851802$, placing the displayed law 2.46 propagated experimental standard uncertainties below it [20]. These comparisons hold the external α fixed and assign no theoretical error. Both are retrospective: the measured ratios were known. A precision prediction requires a derived correction or a justified theoretical uncertainty at the corresponding scale.

7. Cosmological predictions as linked observables

The cosmological realization assigns a closed occupancy φ^{-4} to the present dark-energy channel and identifies its evolution with $a = (1+z)^{-1}$ [21, 10]. Under those physical assignments,

$$d = \varphi^{-4}J(\varphi) = \varphi^{-4}\left(\varphi - \frac{3}{2}\right) = \frac{13\sqrt{5} - 29}{4}, \qquad w(a) = -1 + da. \tag{52}$$

The identity $\varphi^{-1} = \varphi - 1$ makes $J(\varphi) = \varphi - 3/2$: the amplitude is the comparison cost at the hierarchy ratio, multiplied by the stated occupancy. This selects $(w_0, w_a) = (-1+d, -d) \simeq (-0.982779, -0.017221)$ in the usual form $w(a) = w_0 + w_a(1-a)$. The exact line $w_0 + w_a = -1$, the sign of the departure, and the lack of phantom crossing are linked tests of this realization.

Proposition 15 (Density and expansion consequences)**.** *Assume separately conserved dark energy obeys* (52)*. Then*

$$\rho_{\text{de}}(a) = \rho_{\text{de},0}\exp[3d(1-a)]. \tag{53}$$

Assume the standard Einstein–Friedmann equations, spatial flatness, separately conserved pressureless matter, and negligible radiation. Define $H = \dot a/a$, $q = -\ddot a/(aH^2)$ and $j = \dddot a/(aH^3)$. The present values obey

$$q_0 = \frac{1}{2} - \frac{3}{2}\Omega_{\text{de},0} + \frac{3}{2}\Omega_{\text{de},0}d, \qquad j_0 = 1 - 6\Omega_{\text{de},0}d + \frac{9}{2}\Omega_{\text{de},0}d^2. \tag{54}$$

Proof. Conservation gives $d\log\rho_{\text{de}}/d\log a = -3(1+w) = -3da$. Integration from 1 to a proves (53). The flat Friedmann equations give $q = 1/2 + (3/2)\Omega_{\text{de}}w$ and $\Omega'_{\text{de}} = -3w\Omega_{\text{de}}(1-\Omega_{\text{de}})$, where a prime denotes $d/d\log a$. The identity $j = q + 2q^2 - q'$ gives

$$j = 1 + \frac{9}{2}\Omega_{\text{de}}w(1+w) - \frac{3}{2}\Omega_{\text{de}}w'.$$

Substitute $w_0 = -1 + d$ and $w'_0 = d$ to obtain (54). □

Eliminating $\Omega_{\mathrm{de},0}$ from (54) gives a further exact test,

$$\boxed{j_0 - 1 = \frac{d(4-3d)}{1-d}\left(q_0 - \frac{1}{2}\right).} \tag{55}$$

The coefficient is fixed by (52). This relation between acceleration and jerk is independent of the present dark-energy density within the stated cosmological model. The amplitude, equation-of-state slope, density history, and expansion derivatives can therefore be tested jointly. Identifying the dark-energy channel and its clock supplies the physical input (52).

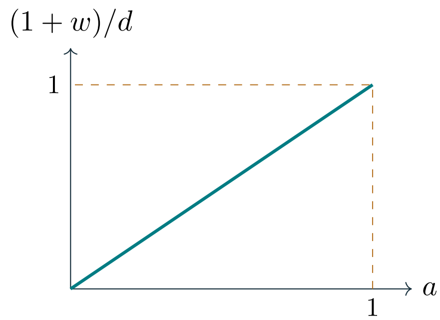

$w(a) = -1 + da$

$\rho_{\mathrm{de}}(a)/\rho_{\mathrm{de},0} = e^{3d(1-a)}$

One law also fixes the density-independent relation between q_0 and j_0 in (55).

Figure 14: The registered dark-energy history. The vertical axis is normalized by the predicted amplitude d. This schematic displays the analytic law; it contains no survey measurements.

The dark-matter realization gives

$$\Omega_{\mathrm{dm}} = \sin(\pi/12) + \frac{\varphi^{-4}}{24} = 0.2648981\ldots$$

from its directed-phase and unresolved-share identifications [22]. The clock-inclusive and pattern-only readings in [10] use thirteen equivalent content channels, twelve visible to the pattern read. With fixed total content c, strict convexity gives equal minimizing shares $s = c/13$. Shared additive readouts therefore have $R_{\mathrm{clock}}/R_{\mathrm{pattern}} = 13s/(12s) = 13/12$ for nonzero content. Identifying these readouts with the late- and early-universe probes gives $H_{\mathrm{late}}/H_{\mathrm{early}} = 13/12$ under that physical assignment. Their comparisons with existing cosmological data are retrospective tests. The dark-energy history and finite-wavelength dispersion can be frozen before new data and tested prospectively. A novel confirmed prediction requires that chronology as well as agreement in the same observable, regime, and uncertainty.

8. The common dynamical realization

The common-functional construction in Section 4 gives a definite interacting realization on a normalized finite state space. Its scalar potential changes matter propagation; covariant matter coherence changes the potential; and the link derivative gives the current appearing in the matter continuity equation. Global field solvability is equivalent to absence of bridges, and complete finite evolution follows under the stated kinetic and temporal identifications. Trivial links select a unique positive ground state, with nonlinear orbital stability and a reversible ground-state transform. The exact phase solution (25) demonstrates a physical consequence internal to this realization that a density-only source law cannot express.

The remaining common-carrier construction must identify this finite dynamics with the charged and geometric sectors, including propagating metric degrees of freedom and their quantum readout. A first-order geometric candidate follows directly from the shared minimum:

$$\mathcal{L}(u, \lambda; q) = \sum_e f(u_e) - \lambda^T(Au - \kappa\delta(q)). \tag{56}$$

Taking the infimum over u gives, where $|(A^T\lambda)_e| \le 1$,

$$\mathcal{L}_{\text{dual}} = \kappa\lambda^T\delta(q) - \sum_e \left[1 - \sqrt{1 - (A^T\lambda)_e^2}\right]. \tag{57}$$

Indeed the convex conjugate of f is $f^*(y) = 1 - \sqrt{1-y^2}$ on $[-1,1]$, with infinite value outside. For finite stationary u the inequality is strict; at $|y| = 1$ the infimum is approached only as $|u| \to \infty$. This is an exact consequence of the finite variational problem, not yet a derived gravitational action.

The area–deficit geometry supplies a sharper guide to the common action. For a closed flat-simplex triangulation, the Schläfli identity gives

$$\sum_h \mathcal{A}_h\, d\delta_h = 0, \qquad dS_R = \sum_h \delta_h\, d\mathcal{A}_h, \qquad \sum_h d\mathcal{A}_h \wedge d\delta_h = 0. \tag{58}$$

The last identity follows by exterior differentiation of the first. Thus the geometric length realization is isotropic in area–deficit phase space, and the one-form $\sum_h \delta_h\, d\mathcal{A}_h$ pulls back to the exact form dS_R. This is a canonical relationship between curvature and area; it does not require every hinge area to be an independent coordinate.

The multiplier λ in (56) is conjugate to prescribed content, which is a different role. At a flat background with $c = 0$, the unique minimum has $u^* = 0$ and, for full row rank, $\lambda = 0$, whereas nondegenerate hinge areas remain positive. A literal identification $\kappa\lambda_h = \mathcal{A}_h$ therefore fails already at the background. A common first-order action must incorporate the area background and the geometric constraints so that its variation yields (58). The constrained response–fluctuation identity in Theorem 3 is an exact part of this construction that already uses one action and one tangent state space.

The physical charged action must supply alternating sources and their long-time poles, select the nonabelian representations, and fix the electric normalization used in Proposition 13. The finite construction already specifies a coupled scalar-field equation, a matter equation, and their shared current. Extending these to a quantum theory of matter and propagating geometry must retain their joint variation. In particular, the relaxed response (30) shows why holding the field fixed in second-order matter response would omit part of the interaction.

The results establish explicit links at both the variational and dynamical levels. One constrained Hessian fixes susceptibility and Gaussian covariance. A field cost and its kinetic Hessian define a common functional with an exact graph solvability criterion, globally conserved dynamics, and phase-sensitive backreaction. Its unique positive ground state links coherent equilibrium to reversible probability transport through one bond conductance. Reciprocal cost also admits an exact normalized-amplitude realization; cycle closure and the quadratic cost recover the Newtonian field; and one geometric spatial operator fixes the two-mode gravitational branch and its relation to light. The charged-source identity and the density-independent cosmological relation add further consistency conditions. The physical common-carrier realization must satisfy these links simultaneously. A decisive empirical test compares a fixed quantitative prediction with an independently measured outcome in the same observable, regime, and uncertainty.

Appendix A. A controlled nonlinear approximation

The shared minimum can be approximated beyond its Hessian without fitting higher-order coefficients. Let A have full row rank, and define

$$v = A^T(AA^T)^{-1}c, \qquad r = \|v\|_2, \qquad Q_4(c) = \frac{r^2}{2} - \frac{1}{8}\sum_e v_e^4.$$

Here v is the minimum-norm feasible vector. The following global bounds make the small-content approximation explicit.

Proposition 16 (Quartic approximation with certified remainder)**.** *For every c,*

$$\sqrt{1+r^2}-1 \le W(c) \le F(v) \le \frac{r^2}{2}, \tag{A.1}$$

$$-\frac{r^6}{8}\left(1+\frac{r^2}{2}\right)^3 \le W(c)-Q_4(c) \le \frac{r^6}{16}. \tag{A.2}$$

A sharper computable lower bound is

$$F(v)-\frac{\eta^2}{2m} \le W(c) \le F(v), \qquad \eta = \|P_{\ker A}\nabla F(v)\|_2, \quad m=(1+r^2/2)^{-3}. \tag{A.3}$$

Proof. For nonnegative a, b, squaring shows $\sqrt{1+a}+\sqrt{1+b} \ge 1+\sqrt{1+a+b}$. Induction gives $F(u) \ge \sqrt{1+\|u\|_2^2}-1$. Every feasible $u = v+z$, $z \in \ker A$, has $v \perp z$, hence norm at least r. Feasibility of v and $\sqrt{1+x^2}-1 \le x^2/2$ prove (A.1).

For the actual minimizer u^*, these bounds imply $\|u^*\|_2^2 \le r^2 + r^4/4$. Along the segment from v to u^*, the Hessian therefore satisfies $\nabla^2 F \succeq (1+r^2+r^4/4)^{-3/2} I = mI$. Strong convexity and $u^*-v \in \ker A$ give

$$F(u^*) \ge F(v) - \eta\|u^*-v\|_2 + \frac{m}{2}\|u^*-v\|_2^2 \ge F(v) - \frac{\eta^2}{2m}.$$

Since $P_{\ker A} v = 0$ and $|f'(x)-x| \le |x|^3/2$, one has $\eta \le r^3/2$. Finally Taylor's integral remainder for $\sqrt{1+y}$, $y \ge 0$, gives

$$0 \le f(x) - \frac{x^2}{2} + \frac{x^4}{8} \le \frac{x^6}{16}.$$

Sum over v_e, use $\sum_e |v_e|^6 \le r^6$, and combine with (A.3) to obtain (A.2). □

The quartic coefficient depends on the same incidence matrix as the quadratic response. The remainder is $O(r^6)$ near equilibrium. When the projected residual η vanishes, (A.3) proves that v is already the exact nonlinear minimum.

CRediT contribution statement

Jonathan Washburn: Conceptualization; Methodology; Writing – original draft. Megan Simons: Writing – review & editing (lead; primary manuscript editor). Recognition Science Team: Writing – review & editing.

References

[1] J. Washburn and M. Zlatanović, Uniqueness of the Canonical Reciprocal Cost, *Mathematics* **14**, 935 (2026). doi:10.3390/math14060935.

[2] S. Pardo-Guerra, J. Washburn and E. Allahyarov, A Coherence Theorem for Conserved Comparison Ledgers: Structural Axioms Pin Down the Scale, the Cost, and the Ratio, *Mathematics* **14**, 2672 (2026). doi:10.3390/math14152672.

[3] S. Pardo-Guerra, A. Thapa, M. Simons and J. Washburn, Coherent Comparison as Information Cost: Axiomatic Foundations for Discrete Ledger Dynamics, *Foundations* **6**, 17 (2026). doi:10.3390/foundations6020017.

[4] A. Thapa and J. Washburn, Finite-Volume Stability and Flux Sectors in a Reciprocal Ratio Gradient Model on Graphs, *Mathematics* **14**, 2726 (2026). doi:10.3390/math14152726.

[5] A. Thapa and J. Washburn, Reciprocal Cost and an Eight-Tick Register: A Conditional Recognition-Operator Construction, *Mathematics* **14**, 3134 (2026). doi:10.3390/math14173134.

[6] M. Simons, E. Allahyarov and J. Washburn, A Discrete Informational Framework for Classical Gravity: Ledger Foundations and Galaxy Rotation Curve Constraints, *Entropy* **28**, 477 (2026). doi:10.3390/e28040477.

[7] J. Washburn, M. Zlatanović and E. Allahyarov, The D'Alembert Inevitability Theorem, *Mathematics* **14**, 1386 (2026). doi:10.3390/math14081386.

[8] J. Washburn, The Golden Hierarchy from Additive Record Updates (2026). doi:10.5281/zenodo.22668480.

[9] S. Pardo-Guerra and J. Washburn, Three Dimensions from a Recognition Requirement (2026). doi:10.5281/zenodo.22680131.

[10] J. Washburn, Quantum Gravity from Ledger Accounting: Shared-Channel Dynamics, Weak-Field Geometry, and Cosmological Readouts (2026). doi:10.5281/zenodo.22668563.

[11] J. Washburn, M. Zlatanović and P. Beltracchi, Multidimensional Cost Geometry, *Axioms* **15**, 378 (2026). doi:10.3390/axioms15050378.

[12] D. Giulini and A. Großardt, Gravitationally induced inhibitions of dispersion according to the Schrödinger–Newton equation, *Classical and Quantum Gravity* **28**, 195026 (2011). doi:10.1088/0264-9381/28/19/195026.

[13] T. Regge, General Relativity without Coordinates, *Il Nuovo Cimento* **19**, 558–571 (1961). doi:10.1007/BF02733251.

[14] M. Roček and R. M. Williams, Quantum Regge Calculus, *Physics Letters B* **104**, 31–37 (1981). doi:10.1016/0370-2693(81)90848-0.

[15] J. Washburn, Gravity and Light on One Lattice (2026). doi:10.5281/zenodo.22680040.

[16] J. Washburn, Record Rules Force Born Probabilities (2026). doi:10.5281/zenodo.22668370.

[17] J. Washburn, The Fine-Structure Constant as a Renormalized Lattice Stiffness (2026). doi:10.5281/zenodo.22676911.

[18] J. Washburn, Cubic Invariant of Charged Fermion Masses (2026). doi:10.5281/zenodo.22680027.

[19] J. Washburn and E. Allahyarov, Charged Lepton Masses from the Recognition Composition Law: A Derivation with Zero Continuously Adjustable Dimensionless Parameters, *Symmetry* **18**, 962 (2026). doi:10.3390/sym18060962.

[20] S. Navas et al. (Particle Data Group), Review of Particle Physics, *Physical Review D* **110**, 030001 (2024). Tau mass listing; muon mass listing.

[21] J. Washburn, A Parameter-Free Prediction for the Present Dark-Energy Equation of State, with the Dilution Law Derived (2026). doi:10.5281/zenodo.22151681.

[22] J. Washburn, The Dark-Matter Fraction from Recognition Closure: A Conditional Derivation (2026). doi:10.5281/zenodo.22151749.